# LAYER-BY-LAYER SELF-ASSEMBLY APPROACH IN THE UV PROTECTIVE MODIFICATION OF ARAMID-BASED MATERIALS

# ARAMİD ESASLI MATERYALLERİN UV KORUYUCU MODİFİKASYONUNDA ÇOK TABAKALI KENDİLİĞİNDEN DÜZENLENME YAKLAŞIMI

Yeşim ÜNVAR[1]
Ayşe Merih SARIIŞIK[1*]
Şule Sultan UĞUR[2]

[1]Dokuz Eylul University, Department of Textile Engineering, Izmir, Turkey
[2]Süleyman Demirel University, Department of Textile Engineering, Isparta, Turkey

**Bu makaleye atıf yapmak için (To cite this article):**

*Araştırma Makalesi / Research Article*

# LAYER-BY-LAYER SELF-ASSEMBLY APPROACH IN THE UV PROTECTIVE MODIFICATION OF ARAMID-BASED MATERIALS

**Yeşim ÜNVAR[1]**
**Ayşe Merih SARIIŞIK[1*]**
**Şule Sultan UĞUR[2]**

[1]Dokuz Eylul University, Department of Textile Engineering, Izmir, Turkey
[2]Süleyman Demirel University, Department of Textile Engineering, Isparta, Turkey

**ABSTRACT:** This paper presents the Layer by Layer self-assembly (LbL) approach for developing the UV resistance of aramid yarns. Initially, a pretreatment was achieved by polyethyleneimine to obtain cationic surface charges on aramid yarns. Then zinc oxide and titanium dioxide nanoparticles were self-assembled on these yarns by the LbL process. The findings revealed that the LbL nano coatings significantly improved the UV resistance and tensile properties of the aramid yarns. This study highlights the unique opportunities offered by the LbL methodology to both modify aramid-based materials in mild conditions and provide an effective UV protection.

*Keywords:* Aramid, UV resistance, Layer by Layer self-assembly, nanocoating

## ARAMİD ESASLI MATERYALLERİN UV KORUYUCU MODİFİKASYONUNDA ÇOK TABAKALI KENDİLİĞİNDEN DÜZENLENME YAKLAŞIMI

*ÖZ:* Bu makale, aramid ipliklerin UV dayanımını geliştirmek üzere çok tabakalı kendiliğinden düzenlenme (LbL) yaklaşımını sunmaktadır. Başlangıçta, aramid iplikler üzerinde katyonik yüzey yükleri elde etmek için polietilenimin ile bir ön işlem gerçekleştirilmiş ve daha sonra bu iplikler üzerinde LbL prosesi ile çinko oksit ve titanyum dioksit nano parçacıkları kendiliğinden düzenlenmiştir. Bulgular, LbL nano kaplamaların aramid ipliklerin UV direncini ve çekme özelliklerini önemli ölçüde artırdığını ortaya koymuştur. Bu çalışma, LbL metodolojisinin hem aramid esaslı materyalleri ılıman koşullarda modifiye etme hem de etkili bir UV koruması sağlama konusunda sunduğu benzersiz fırsatları vurgulamaktadır.

*Anahtar Kelimeler:* Aramid, UV dayanımı, Çok tabakalı kendiliğinden düzenlenme, nano kaplama

# 1. INTRODUCTION

Aramid fibers possess many superior properties like ultra-high strength and modulus, lightweight, good thermal and chemical resistance; and their outstanding integrated performances render them one of the best competitors meeting harsh requirements in numerous cutting-edge fields like space and aviation, defense, and electronics [1-5]. However, when exposed to UV light, aramid fibers undergo rapidly evolving photolytic/ photooxidative reactions, which result in wear, discoloration, and loss of thermal and mechanical properties [6-11]. The poor UV resistance shortens the outdoor service life of aramid fibers and greatly restricts their applications [12, 13]. Moreover, considering it is an indispensable strategic material for national security, construction, and scientific and technological progress [13], UV-induced strength losses are unacceptable. Therefore, eliminating or minimizing these damages with UV protective coatings is of great interest both in academia and industry.

Nevertheless, the main problem of coating aramid fibers is their chemically inert surface, originating from strong conjugation and steric hindrance within the molecular chain [14]. This critical drawback transforms even an ordinary coating process into a significantly challenging task and also limits the effectiveness of UV protective coatings on these fibers [14-16.] Hence, aramid fibers are pretreated with mostly acid or alkali prior to any surface treatment [1, 2, 4]. In fact, any attempt to modify aramid fibers entails highly demanding operational requirements including high temperature and/or pressure, prolonged and complicated processes, and the necessity for exploiting specific machinery depending on the modification method [4, 12-18]. However, it is essential to note that abrasive pretreatments destroy the structural integrity and tensile properties of aramid fibers [5]. Therefore, the real challenge lies not only in developing an effective UV protective coating but also in seamlessly integrating it without compromising the intrinsic properties of aramid fibers.

In this regard, the Layer by Layer (LbL) self-assembly approach offers a promising solution to these challenges as an easy, efficient, reproducible, robust, and versatile bottom-up strategy to modify surfaces and prepare functional coatings [19]. LbL self-assembly, particularly driven by electrostatic interactions, is by far the most extensive and powerful way of constructing LbL films; it relies solely on the alternating adsorption of oppositely charged particles and enables the use of a wide range of materials [19]. Upon its exceptional versatility, LbL methodology holds the great potential to surpass restrictions related to substrate properties or even render them inconsequential. Notably, the pioneering works by Uğur and co-workers on the application of LbL for textile surfaces, particularly utilizing nanoparticles, have revealed unexplored potential [20-23]. Although LbL offers a valuable opportunity to tailor the surface properties of textile fibers, its utilization in modifying aramid fibers remains surprisingly scarce [24-28], with only two studies focusing on UV protection [4, 29].

Concerning the limited use of LbL, it can be addressed that inorganic one-dimensional UV absorbers, such as $TiO_2$ and ZnO nanoparticles, may not be suitable for modifying aramid fibers due to their (i) photocatalytic activities and (ii) limited surface coatings [4]. The first point seems plausible, indeed semiconductors pose a risk of damaging the substrate itself [30, 31]. As for the second point, the relatively limited surface area of nanoparticles could be quite discouraging for adopting LbL in UV protection as it is a surface phenomenon, and effective coverage of the fiber surface is crucial. As a result, the risks and difficulties in coating aramid fibers, coupled with the fact that LbL is mainly applied to relatively easy-to-process fibers such as cotton and polyester [32], may have created a prevailing notion over time that LbL is an unsuitable method for modifying aramid fibers. Taken together, solid reasoning for the limited use of LbL becomes evident.

Discussing UV protection, it is essential to consider the UV aging treatments as they reveal the effectiveness of the coatings. While UV protection is mainly developed against UVA and/or UVB rays, certain applications like aviation and welding operations [33, 34] require protection against UVC rays as well. Besides, UVC irradiation has gained great interest in neutralizing biological threats, such as coronaviruses [35-37]. Due to the rising demand for disinfection and sterilization, UVC technology has been integrated into various devices and everyday objects, becoming ubiquitous. Thus, accounting for UVC light in the assessment of UV protective coatings can become necessary in the near future, and in certain fields, it could be imperative. However, protective additives against UVC radiation and their effects on materials in our daily lives remain largely unknown [38].

This study was carried out to explore the possibilities of the Layer by Layer self-assembly approach in UV protective modifications of aramid-based materials. Overcoming existing limitations, we aimed to establish an effective and simple coating process. To achieve this, we conducted a mild pretreatment using polyethyleneimine to introduce cationic charges on the fiber surface. This allowed us to overcome the chemically inert surface of aramid fibers and create an appropriate sublayer for the subsequent LbL self-assemblies. Harnessing the charged surface, we successfully coated aramid fibers with $TiO_2$ and ZnO nanoparticles. Advanced protection in a harsh environment of highly energetic UVC rays validated the effectiveness of LbL coatings. This research uncovered the strong potential of LbL technology to overcome limitations in the UV protective modifications of aramid-based materials and establish a sustainable alternative to current practices.

# 2. MATERIAL AND METHOD

## 2.1. Material

Para-aramid (Kevlar 49) staple yarns (60/1 Nm, Z twist) were kindly supplied by Kipaş Textiles. Polyethylenimine (branched,

average Mw ~25,000) and TiO$_2$ and ZnO nanoparticles were purchased from Sigma-Aldrich. Sodium hydroxide (NaOH) and hydrochloric acid (HCl) were used for pH adjustment.

## 2.2. Method

### 2.2.1. Pretreatment

Polyethyleneimine (PEI) is a common cationic polyelectrolyte in electrostatic self-assembly with strong adhesion, and recent applications have shown that it can serve as a suitable template to overcome chemically inert surfaces [32, 39, 40]. Based on this, pretreatment was carried out using PEI to obtain cationic charges on aramid yarns. Aramid yarns were immersed in the PEI solution (1 g/L) for 20 min and then dried without any heat treatment.

### 2.2.2. UV Protective LbL Coatings

Aqueous anionic and cationic dispersions of ZnO and TiO$_2$ (1 g/L) were prepared using an ultrasonic homogenizer (Hielchier, 40 W, 26 kHz) and adjusting pH with NaOH and HCl, respectively. After the pretreatment with PEI, aramid yarns were dipped first into anionic dispersions of ZnO or TiO$_2$ (20 minutes) and then into cationic dispersions, and washed in each sequential step (5 minutes). At the end of this cycle, a bilayer of ZnO or TiO$_2$ nanocoating was obtained. Ten layers of LbL nanocoating were obtained by repeating this cycle five times at room temperature for each and then drying at 105 °C for 5 minutes. The entire process is depicted in Figure 1.

### 2.2.3. Accelerated UV Aging

Regarding UVC aging, test method development at global standards organizations, such as ASTM and ISO, is still in its early stages, and commercial UVC testing instruments are relatively new [38]. Therefore, without relying on a standard like others [41, 42], we conducted accelerated UV aging in a self-designed box (60 cm x 60 cm x 60 cm) using three Philips TUV series 253.7 nm UVC lamps (model: 15W15G8T, 41 cm long) for 168 hours.

### 2.2.4. Characterizations and Tests of UV Protective LbL Coatings

The morphologies of the aramid yarns were observed using a Carl Zeiss 300VP Scanning Electron Microscope (SEM). The aramid yarns were tested in Attenuated Total Reflection Infrared (ATR-FTIR) mode using a Thermo Scientific Nicolet iS50 FTIR Spectrometer, with a wave number range of $400 \sim 4000$ cm$^{-1}$. To assess the UV protection efficiency of LbL nanocoatings, tensile strength, and break extension were measured according to TS EN ISO 2062 before and after UV aging.

## 3. RESULTS AND DISCUSSION

### 3.1. SEM Observation

SEM images of the aramid yarns taken at ×2500 and ×5000 magnifications are displayed in Figure 2 for a-b) untreated, c-d) PEI pretreatment, e-f) ZnO nanocoating, and g-h) TiO$_2$ nanocoating. The average diameter of the aramid fiber was approximately 12 µm. Some narrow grooves are uniformly distributed in the longitudinal direction of the fiber, indicating axial orientation [43, 44]. The punctiform stains generated during the production of fibers are also observed [40]. Additionally, there are some fibrillar structures misaligning to the fiber axis with diameters mostly below 1 µm, and some appear to be roughly 200-400 nm in size. It was observed that some fibrillar structures seemed to peel off of the fiber's skin layer in the longitudinal direction, while others appeared as a single solid piece (Figure 2a). Furthermore, some formed continuous ribbons that coiled into helices (clearly visible in Figure 2e, f) [43]. The presence of these separated fibrillar structures in SEM images suggests that certain microfibrils may have become detached from the fiber structure during the manufacturing process. The fibrous form consisting of staple fibers might have contributed to these splittings, as they presumably tended to create broken fiber ends and separate into microfibrils [44, 45]. Yet, further analysis, such as advanced microscopy techniques and material testing, would be required to study the exact nature and implications of these microfibril observations in Kevlar fibers. These observations thus need to be interpreted with caution and closer inspection.
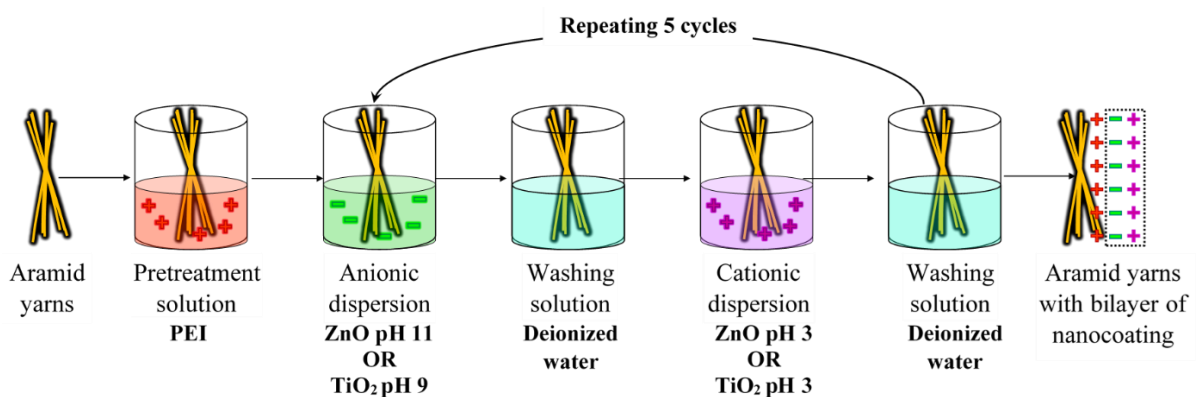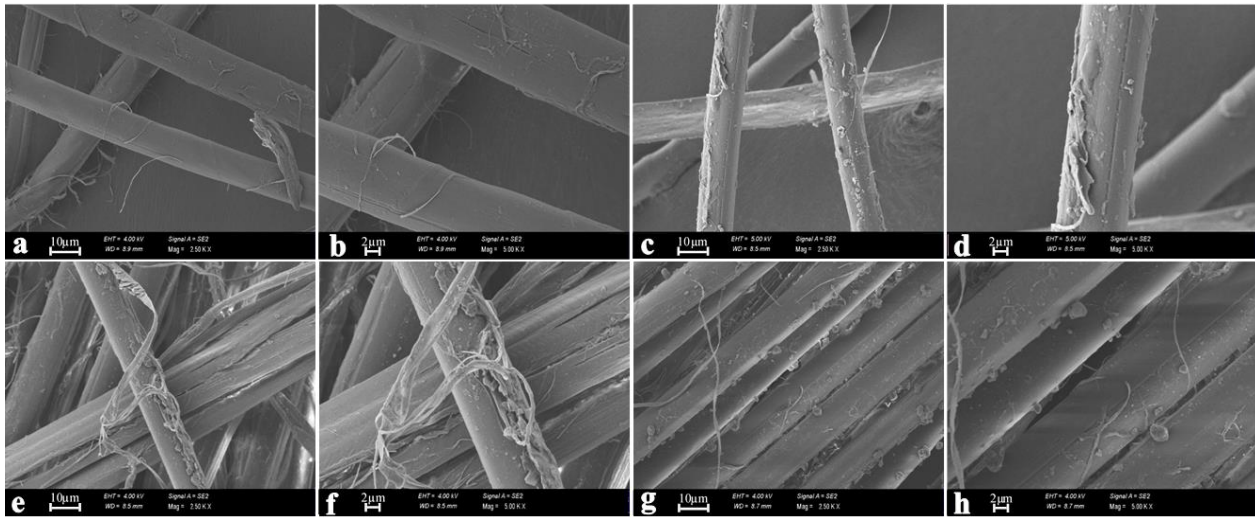


**Figure 1.** Pretreatment and LbL nanocoatings of aramid yarns

**Figure 2.** SEM micrographs of aramid yarns; a,b) untreated, c,d) PEI pretreatment, e,f) ZnO nanocoating, g,h) TiO₂ nanocoating (In the ordered pair, the first letters represent x2500, while the latter ones represent x5000)

Apart from the fibrillar structure, the untreated fiber surface appeared smooth and clean, whereas an attached dense coating layer was observed after the PEI pretreatment (Figure 2c, 2d). However, the PEI coating exhibited uneven distribution, with some regions showing abundance (Figure 2e, 2f), while others had a relatively thin and uniform layer (Figure 2g, 2h). The non-uniformity of the PEI coating appeared to affect the distribution of nanoparticles, as well. ZnO nanoparticles tended to agglomerate, whereas TiO₂ nanoparticles were smaller, evenly distributed, and separated. While it was not expected to achieve full coverage of fibers with LbL coatings, as in the case of atomic layer deposition [12, 14], it was also not predicted that the PEI coating would show relatively moderate to high levels of differences in region to region. These observations imply two points about exploiting a strong adhesive material serving as a charged sublayer for subsequent LbL coatings. This surface strategy might be more effective in the implementation of nanoparticles in case: providing a uniform and widely spread sublayer coating, which would enable well-manipulated and controlled distributions of particles, or simply using UV absorbers with a larger surface area, as suggested [4].

Regarding the fact that this was only a preliminary attempt to coat aramid fibers with a simple and easy approach, it is hardly surprising that LbL coatings were imperfectly distributed along the fiber. It should be reminded that no chemicals other than PEI were exploited, and even heat treatments were not applied after PEI coating. Likewise, LbL coatings were carried out without drying between each self-assembly deposition, contrary to previous studies [4, 27, 29]. Although the surface coverage performance appeared to be not ideal, we nevertheless believe that LbL has strong potential for the deposition of nanocoatings with the right material combination, and provides a unique opportunity to tailor the surface of fibers, even inert ones like aramid.

## 3.2 ATR-FTIR Analysis

Figure 3 displays the ATR-FTIR measurement results of untreated and LbL-coated aramid yarns before and after UV aging. The FTIR spectra show specific amide-related peaks at certain wavenumbers: 3308 cm⁻¹ (amide A), 1642 cm⁻¹ (amide I), 1537 cm⁻¹ (amide II), 1298 cm⁻¹ and 1223 cm⁻¹ (amide III), and 721 cm⁻¹ (amide IV) [11, 27, 46-49]. Additionally, bands at 817 cm⁻¹ indicate out-of-plane C-H vibrations of two adjacent hydrogens in an aromatic ring, while 521 cm⁻¹, 720 cm⁻¹, and 805 cm⁻¹ bands suggest out-of-plane N-H deformation modes, indicating para disubstitution in the aromatic ring [50, 51]. The absorption bands at 1510 cm⁻¹, 1014 cm⁻¹, and 817 cm⁻¹ are attributed to the C–H deformation of the aromatic ring [52], and the band at 1605 cm⁻¹ is related to the C=C tensile vibration of the benzene ring [12, 50, 53].
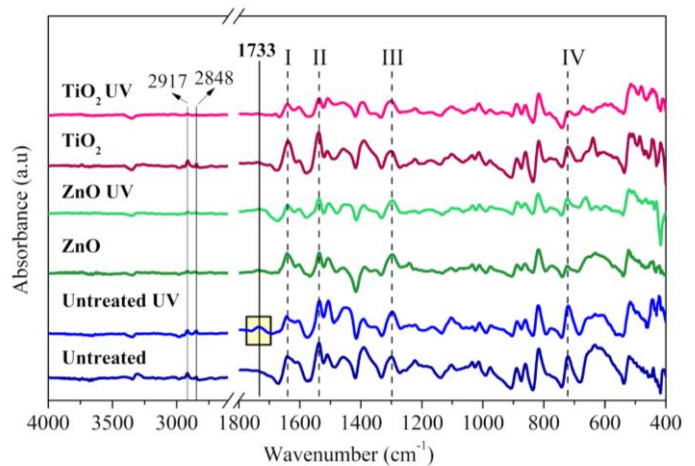


**Figure 3.** ATR-FTIR analysis of aramid yarns

The bands at 2917 cm⁻¹ and 2848 cm⁻¹ are associated with the stretching of C–H groups, as well as aldehyde groups [54]. Previous studies have linked these bands to the incorporation of PEI [27, 55], indicating effective PEI coating on $TiO_2$-coated yarns, as evidenced by strong peaks. However, in the spectrum of ZnO-coated yarns, these bands appear weak, possibly due to the nonuniform PEI coating mentioned in SEM. Normally, these peaks could indeed be observed [13, 54, 56]. Nevertheless, their unusually high intensity in our study raises the possibility that they may result from the residual sizing agent used in the manufacturing process. It is worth considering that aramid yarns were not thoroughly cleaned in a harsh medium containing acid [57], which might explain the observed peak intensity. Despite this, we successfully achieved our goal of avoiding the use of harsh treatments and directly coated the aramid fibers.

In the case of ZnO-coated samples, specific peaks at 425 cm⁻¹, 450 cm⁻¹, and 570 cm⁻¹ are associated with the characteristic Zn-O stretching vibration [58-60]. Furthermore, the peaks observed at 1242 cm⁻¹, 1350 cm⁻¹, and 1736 cm⁻¹ might suggest the presence of ZnO coating on aramid yarns, as they are specifically detected in the FTIR spectra of ZnO-coated samples. In the case of $TiO_2$-coated yarns, a broad absorption band observed roughly at 400-700 cm⁻¹ is attributed to the bending vibrations of the Ti-O and -O-Ti-O groups, which is clearly visible in the figure. Additionally, there are distinct peaks at 417 cm⁻¹ (in-plane TiOH bending) and 485 cm⁻¹ (out-of-plane TiOH bending), as well as 639 cm⁻¹ (sym-TiOH stretching), all of which are related to $OTi(OH)_2$ [61]. Moreover, the peak at 1123 cm⁻¹ can be linked to the formation of amide linkages between aramid yarns and $TiO_2$.

After UV irradiation, changes in intensities were observed in the IR spectra. Reduction in the intensities of the Amide I, II, and III peaks was noticed, indicating potential damage to the polymer backbone and the formation of carboxylic acids and other oxidized species, likely due to photo-oxidation [11, 62]. Furthermore, shouldering peaks at 1605 cm⁻¹ and 1510 cm⁻¹ tended to converge with amide I and II, respectively. After UV aging, the peak at 1350 cm⁻¹ remains, while the other peaks that presumably indicate the amide-ZnO linkage (1242 cm⁻¹ and 1736 cm⁻¹) disappear. This observation may suggest the degradation of the amide-related bonds in the aramid yarns due to UV exposure. The increase in the intensity of the C=O stretch peak (1102 cm⁻¹) suggests the oxidation of amide groups in the aramid yarns [63]. The peak at 1123 cm⁻¹ combined with the 1102 cm⁻¹ peak after UV aging, indicating possible UV-induced damage for $TiO_2$-coated yarns.

Additionally, after accelerated UV aging, a new peak at 1733 cm⁻¹ appeared in the untreated samples ("untreated UV" indicated in a rectangular yellow box"), which is attributed to the breaking of the amide bond and the formation of a carboxylic acid group [4, 11, 12, 53, 64]. However, no strong peak corresponding to the cleavage of the amide bond was observed in ZnO and $TiO_2$-coated samples after UV aging. This suggests that the coatings may have provided some protection against UV-induced degradation of the amide bonds in the aramid yarns.

The presence of additional ZnO and $TiO_2$ related peaks in the spectrum of coated samples indicates the successful achievement of LbL nanocoatings. The FTIR spectrum showed that UVC aging conditions led to the formation of new functional groups and changes in the intensity of main wave numbers with slight shifts after aging. Despite the somewhat disappointing coating performance, it is surprising that ZnO and $TiO_2$ nanoparticles demonstrated a significant ability to prevent chain scission, especially at 1733 cm⁻¹. This finding suggests that the LbL self-assembly of nanoparticles can be highly effective for UV protection modification of aramid yarns

### 3.3. Tensile Strength and Break Extension Tests

The tensile strength and break extension of aramid yarns before and after UV aging are presented in Figure 4a and 4b, respectively. The tensile properties of the bare para-aramid staple yarn were lower (9.7 cN/dtex; 4.4%) compared to values reported in the literature (20.8 cN/dtex; 2.4%) [44]. As previously observed in the SEM micrographs, the presence of detached fibrillar structures, which are assumed to result from the manufacturing process, might have contributed to the lower tensile properties. Ultimately, these defects could have led to failure by axial splitting, possibly triggered by the shear stresses in a twisted fiber [45]. However, it is worth noting that the coatings were applied to the same yarns, ensuring a consistent assessment of the coatings' effects on the tensile properties.
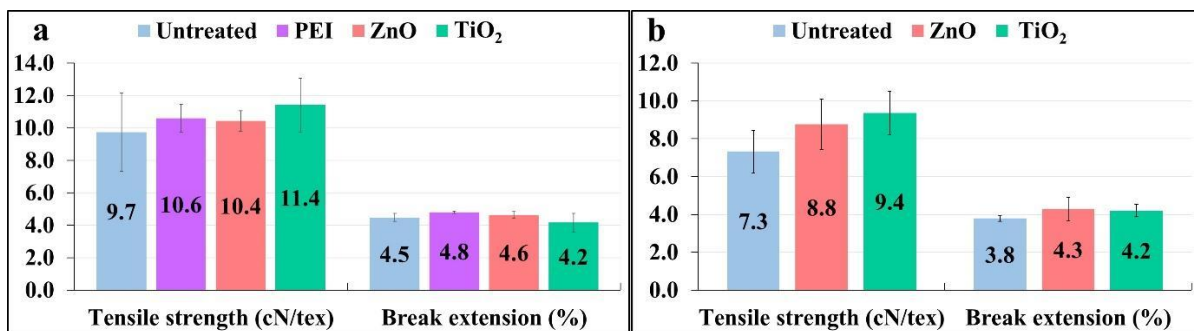


**Figure 4.** Tensile strength and break extension of aramid yarns a) before UV aging b) After UV aging

The tensile strength of the untreated aramid yarn increased by 9%, 7%, and 17% with PEI, ZnO, and TiO$_2$ coatings, respectively. This improvement can be attributed to the beneficial effects of the PEI polymer layer, which introduces active sites to the fiber surface through nondestructive functionalization and helps to repair defects on the fiber surface [55]. It is reasonable to assume that TiO$_2$ performed better than ZnO due to possibly achieving a more uniform coating, as mentioned in the previous subsection. In contrast to some studies that reported only minor changes in tensile strength for ZnO and TiO$_2$-modified fibers [42, 58, 65], our results are quite satisfactory, showing a significant increase in tensile strength. This improvement is particularly notable as previous studies have indicated a decrease in tensile strength for ZnO and TiO$_2$-modified fibers [18, 66-68]. It is worth mentioning that achieving an enhanced tensile strength of aramid fibers after modification is a rare finding [12, 14]. Regarding the break extension, there was a slight decrease observed in TiO$_2$-coated fibers, while the other coatings showed a slight increase. However, these fluctuations can be considered as insignificant since they resulted in an extension of less than 5% [44].

The tensile strength of all aramid yarns decreased after accelerated UV aging (Figure 4b), with untreated yarns showing the most severe decline. It is reasonable to observe a decrease in the break extension of untreated and ZnO-coated yarns, as UV aging may have made the fibers more brittle. However, the break extension of TiO$_2$ nanocoating showed no change. It is important to remind that this preliminary study conducted UV aging solely with a UVC lamp, without considering the additional effects of temperature and moisture. For more realistic simulations, temperature and humidity should be included as essential parameters, as previous studies have shown that UV aging can become extremely severe under such conditions [12, 14, 56]. Although our test conditions were not severely harsh, UVC light energy is higher than UVA and UVB. Therefore, these findings are not unexpected, given the high sensitivity of aramid fibers to UV light.

To assess the UV protection efficiency of LbL nanocoatings more clearly, examining the retention rates of the yarns is beneficial. Tensile strength retentions and break extensions (%) of aramid yarns after 168 hours of UV irradiation were evaluated both individually and in comparison to the untreated yarn, as presented in Figure 5. The break extension retentions of ZnO and TiO$_2$ modified yarns were found to be 92-100% individually or compared to the untreated sample 96-95%, respectively. These findings suggest that the LbL nanocoatings preserved the break extension properties of the aramid yarns after UV aging.

The untreated aramid yarn retained only 75% of its original tensile strength, which is typical for Kevlar49 fibers. In contrast, aramid yarns with ZnO and TiO$_2$ LbL nanocoatings maintained at least 84% and 82% of their original values, respectively. These retention values were obviously higher compared to the untreated sample. It is essential to note that retention rates should be given with reference to the initial values of both the original fiber and the modified fiber; otherwise, the interpretation could be misleading. For instance, the tensile strength of TiO$_2$-coated yarns before and after UV aging was 11.4 cN/tex and 9.4 cN/tex, respectively, resulting in tensile strength retention of 82%. However, when compared to the untreated para-aramid yarns before UV aging (9.7 cN/tex), this value (9.4 cN/tex) corresponds to 96%, which is significantly higher than the 75% retention of the uncoated yarns (7.3 cN/tex), indicating remarkable UV protection.

In previous studies [1-5, 17, 66] that used Kevlar49 fibers and conducted UV aging for 168 hours, the reported UV protection rates ranged from 82% to 97%. Our findings demonstrate that LbL nanocoatings considerably retain the tensile strength of aramid fibers, whether considered individually (82-84%) or compared to the untreated sample (90-96%). This is quite surprising, given the observed incomplete coverage of the fiber surface and the photocatalytic nature of ZnO and TiO$_2$ nanoparticles.
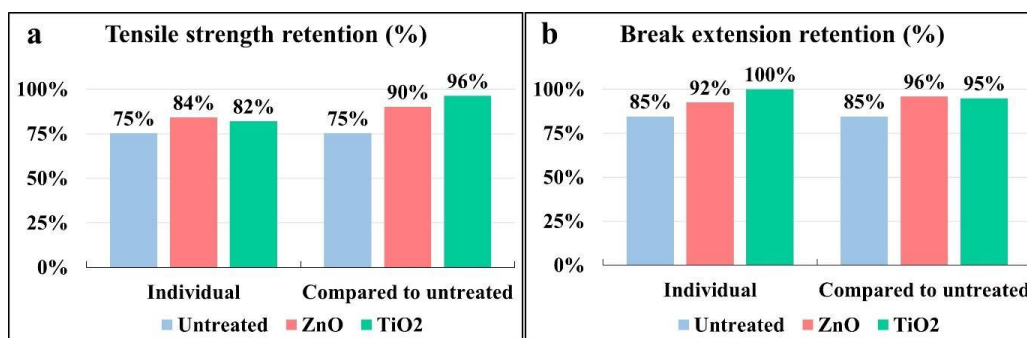


**Figure 5.** Tensile strength (a) and break extension (b) retentions of aramid yarns after UV aging

## 4. CONCLUSION

This paper presents the Layer by Layer self-assembly approach for assessing its potential in the UV protective modifications of aramid-based materials. Prior to the application of LbL nanocoatings, a PEI coating was carried out to create a charged sublayer. This approach facilitated overcoming the inert nature of aramid fibers while circumventing the need for abrasive pretreatments. The findings showed that the LbL technique enables the self-assembly of ZnO and TiO$_2$ nanoparticles on PEI-coated aramid yarns. Tensile strength values of aramid yarns were considerably increased by both PEI pretreatment and LbL nanocoatings. This suggests that it is quite possible to build up nano coatings without compromising the tensile properties of aramid fibers using the LbL approach. Furthermore, LbL nanocoated yarns have significantly preserved their tensile properties after accelerated UVC aging. It was concluded that the LbL self-assembly approach may well overcome the limitations of the current coating practices and is highly suitable for achieving high protection rates in the UV protective modification of aramid-based materials. Indeed, comprehensive investigations need to be conducted to broaden the opportunities offered by LbL and to develop a robust and sustainable UV protection system for aramid fibers. Further LbL applications providing protection against the entire UV spectral range are currently in the development stage, and we hope to share them soon.

## REFERENCES

1. Zhu, X., Yuan, L., Liang, G., & Gu, A., (2014), *Unique UV-resistant and surface active aramid fibers with simultaneously enhanced mechanical and thermal properties by chemically coating Ce 0.8 Ca 0.2 O 1.8 having low photocatalytic activity*, Journal of Materials Chemistry A, 2(29), 11286-11298.

2. Zhang, H., Liang, G., Gu, A., & Yuan, L., (2014), *Facile preparation of hyperbranched polysiloxane-grafted aramid fibers with simultaneously improved UV resistance, surface activity, and thermal and mechanical properties*, Industrial & Engineering Chemistry Research, 53(7), 2684-2696.

3. Zhu, X., Yuan, L., Liang, G., & Gu, A., (2015), *Unique surface modified aramid fibers with improved flame retardancy, tensile properties, surface activity and UV-resistance through in situ formation of hyperbranched polysiloxane–Ce 0.8 Ca 0.2 O 1.8 hybrids*, Journal of Materials Chemistry A, 3(23), 12515-12529.

4. Zhou, L., Yuan, L., Guan, Q., Gu, A., & Liang, G., (2017), *Building unique surface structure on aramid fibers through a green layer-by-layer self-assembly technique to develop new high performance fibers with greatly improved surface activity, thermal resistance, mechanical properties and UV resistance*, Applied Surface Science, 411, 34-45.

5. Zhu, J., Yuan, L., Guan, Q., Liang, G., & Gu, A., (2017), *A novel strategy of fabricating high performance UV-resistant aramid fibers with simultaneously improved surface activity, thermal and mechanical properties through building polydopamine and graphene oxide bi-layer coatings*, Chemical Engineering Journal, 310, 134-147.

6. Carlsson, D. J., Gan, L. H., Wiles, D. M., (1978), Photodegradation of aramids. I. Irradiation in the absence of oxygen, Journal of Polymer Science: Polymer Chemistry Edition, 16 (9), 2353-2363.

7. Carlsson, D. J., Gan, L. H., Wiles, D. M., (1978), *Photodegradation of aramids. II. Irradiation in air*, Journal of Polymer Science: Polymer Chemistry Edition, 16 (9), 2365-2376.

8. Brown, I. M., Sandreczki, T. C., (1982), *Characterization of Kevlar 49 fibers by electron paramagnetic resonance*, Final report, 20 May 1981-20 June 1982, Radicals induced by ultraviolet or fracture, No. UCRL-15512; MDC-Q-0775. McDonnell Douglas Research Labs., St. Louis, MO (USA).

9. Brown, J. R., Browne, N. M., Burchill, P. J., Egglestone, G. T., (1983), *Photochemical ageing of Kevlar® 49*, Textile Research Journal, 53 (4), 214-219.

10. Said, M. A., Dingwall, B., Gupta, A., Seyam, A. M., Mock, G., & Theyson, T., (2006), *Investigation of ultra violet (UV) resistance for high strength fibers*, Advances in space research, 37(11), 2052-2058.

11. Zhang, H., Zhang, J., Chen, J., Hao, X., Wang, S., Feng, X., & Guo, Y., (2006), *Effects of solar UV irradiation on the tensile properties and structure of PPTA fiber*, Polymer degradation and stability, 91(11), 2761-2767.

12. Zhai, L., Huang, Z., Luo, Y., Yang, H., Xing, T., He, A., ... & Chen, F., (2022), *Decorating aramid fibers with chemically-bonded amorphous TiO2 for improving UV resistance in the simulated extreme environment*, Chemical Engineering Journal, 440, 135724.

13. Sun, H., Kong, H., Ding, H., Xu, Q., Zeng, J., Jiang, F., ... & Zhang, Y., (2020), *Improving UV resistance of aramid fibers by simultaneously synthesizing TiO2 on their surfaces and in the interfaces between fibrils/microfibrils using supercritical carbon dioxide*, Polymers, 12(1), 147.

14. Chen, F., Zhai, L., Yang, H., Zhao, S., Wang, Z., Gao, C., ... & Xu, W., (2021), *Unparalleled armour for aramid fiber with excellent UV resistance in extreme environment*, Advanced Science, 8(12), 2004171.

15. Onggar, T., Häntzsche, E., Hund, R. D., & Cherif, C., (2018), *Multiple functional coating highly inert fiber surfaces of para-aramid filament yarn*, Materials Research Express, 5(9), 095702.

16. Sun, Y., Liang, Q., Chi, H., Zhang, Y., Shi, Y., Fang, D., & Li, F., (2014), *The application of gas plasma technologies in surface modification of aramid fiber*, Fibers and Polymers, 15, 1-7.

17. Cai, H., Shen, D., Yuan, L., Guan, Q., Gu, A., Liang, G., (2018), *Developing thermally resistant polydopamine@ nano turbostratic BN@ CeO2 double core-shell ultraviolet absorber with low light-catalysis activity and its grafted high performance aramid fibers*, Applied Surface Science, 452, 389-399.

18. Ma, L., Zhang, J., & Teng, C., (2020), *Covalent functionalization of aramid fibers with zinc oxide nano-interphase for improved UV resistance and interfacial strength in composites*, Composites Science and Technology, 188, 107996.

19. Borges, J., & Mano, J. F., (2014), *Molecular interactions driving the layer-by-layer assembly of multilayers*, Chemical reviews, 114(18), 8883-8942.

20. Ugur, Ş. S., Sariişik, M., & Aktaş, A. H., (2010), *The fabrication of nanocomposite thin films with TiO2 nanoparticles by the layer-by-layer deposition method for multifunctional cotton fabrics*, Nanotechnology, 21(32), 325603.

21. Uğur, Ş. S., Sarıışık, M., Aktaş, A. H., Uçar, M. Ç., & Erden, E., (2010), *Modifying of cotton fabric surface with nano-ZnO multilayer films by layer-by-layer deposition method*, Nanoscale research letters, 5, 1204-1210.

22. Uğur, Ş. S., Sarıışık, M., & Aktaş, A. H., (2011), *Nano-Al2O3 multilayer film deposition on cotton fabrics by layer-by-layer deposition method*, Materials Research Bulletin, 46(8), 1202-1206.

23. Uğur, Ş. S., Sarıışık, M., & Aktaş, A. H., (2011), *Nano-TiO 2 based multilayer film deposition on cotton fabrics for UV-protection,* Fibers and polymers, 12, 190-196.

24. Sui, X., Gao, L., & Yin, P., (2014), *Shielding Kevlar fibers from atomic oxygen erosion via layer-by-layer assembly of nanocomposites*, Polymer degradation and stability, 110, 23-26.

25. Yang, M., Zhang, Z., Yuan, J., Wu, L., Zhao, X., Guo, F., ... & Liu, W., (2020), *Fabrication of PTFE/Nomex fabric/phenolic composites using a layer-by-layer self-assembly method for tribology field application*, Friction, 8, 335-342.

26. Yang, M., Zhang, Z., Wu, L., Li, P., Jiang, W., & Men, X., (2019), *Enhancing interfacial and tribological properties of self-lubricating liner composites via Layer-by-Layer self-assembly MgAl-LDH/PAMPA multilayers film on fibers surface*, Tribology International, 140, 105887.

27. Li, Z., Liu, B., Kong, H., Yu, M., Qin, M., & Teng, C., (2018), *Layer-by-layer self-assembly strategy for surface modification of aramid fibers to enhance interfacial adhesion to epoxy resin*, Polymers, 10(8), 820.

28. Zhang, H., Wu, S., Zhang, Y., Mao, Z., Zhong, Y., Sui, X., ... & Zhang, L., (2023), *Fabrication of Fe-BTC on aramid fabrics for repeated degradation of isoproturon*, Environmental Science and Pollution Research, 30(12), 35214-35222.

29. Nejman, A., Baranowska-Korczyc, A., Ranoszek-Soliwoda, K., Jasińska, I., Celichowski, G., & Cieślak, M., (2022), *Silver Nanowires and Silanes in Hybrid Functionalization of Aramid Fabrics*, Molecules, 27(6), 1952.

30. Fajzulin, I., Zhu, X., Möller, M., (2015), *Nanoparticulate inorganic UV absorbers: a review*, Journal of Coatings Technology and Research, 12 (4), 617-632.

31. Yasukawa, A., Tamura, J., (2021), *Preparation and structure of titanium-cerium-calcium hydroxyapatite particles and their ultraviolet protecting ability*, Colloids and Surfaces A: Physicochemical and Engineering Aspects, 609, 125705.

32. Türkaslan, S. S., Ugur, Ş. S., Türkaslan, B. E., & Fantuzzi, N., (2022), *Evaluating the X-ray-shielding performance of graphene-oxide-coated nanocomposite fabric*, Materials, 15(4), 1441.

33. Mäkinen, H., Karkkula, S., Jaakkola, K., & von Nandelstadh, P., (2004), *Can laboratory pre-treatment of welders' protective clothing simulate their aging process in normal use?*, Journal of ASTM International, 1(5), 1-11.

34. Karahan, H. A., Demir, A., & Toprakçı, O., (2008), *Textile materials and structures used for aerospace applications-1*, Fibers. Electronic Journal of Textile Technologies, 2, 45-65.

35. Bhardwaj, S. K., Singh, H., Deep, A., Khatri, M., Bhaumik, J., Kim, K. H., & Bhardwaj, N., (2021), *UVC-based photoinactivation as an efficient tool to control the transmission of coronaviruses*, Science of The Total Environment, 792, 148548.

36. Olcay, A., Albayrak, S. B., Aktürk, İ. F., Akbülbül, M. C., Yolay, O., İkitimur, H., & Bayer, M. Ç., (2021), *A new Far-UVC based method for germ free hospitals and travel: Initus-V*, medRxiv.

37. Vatansever, F., Ferraresi, C., de Sousa, M. V. P., Yin, R., Rineh, A., Sharma, S. K., & Hamblin, M. R., (2013), *Can biowarfare agents be defeated with light?*, Virulence, 4(8), 796-825.

38. McGreer, M., (2021), *Testing the effects of UV-C radiation on materials*, IST International Surface Technology, 14(2), 46-47.

39. Xiong, M., Ren, Z., & Liu, W., (2019), *Fabrication of UV-resistant and superhydrophobic surface on cotton fabric by functionalized polyethyleneimine/SiO2 via layer-by-layer assembly and dip-coating*, Cellulose, 26(16), 8951-8962.

40. Yang, X., Tu, Q., Shen, X., Pan, M., Jiang, C., Zhu, P., ... & Hu, C., (2019), *Surface modification of Poly (p-phenylene terephthalamide) fibers by polydopamine-polyethyleneimine/graphene oxide multilayer films to enhance interfacial adhesion with rubber matrix*, Polymer Testing, 78, 105985.

41. Lu, Z., Li, D., & Yuan, Z., (2022), *Polypyrrole coating on aramid fabrics for improved stab resistance and multifunction*, Journal of Engineered Fibers and Fabrics, 17, 15589250221081856.

42. Naveen, R., & Kumar, M., (2023), *Enhancing UV resistance of TiO2 reinforced Kevlar 29 fiber using sol-gel & low-temperature hydrothermal processes*, Polymer-Plastics Technology and Materials, 62, 117-128.

43. Morgan, R. J., Pruneda, C. O., & Steele, W. J., (1983), *The relationship between the physical structure and the microscopic deformation and failure processes of poly (p‐phenylene terephthalamide) fibers*, Journal of Polymer Science: Polymer Physics Edition, 21(9), 1757-1783.

44. Hearle, J. W. S., (2001), *High-performance fibres*, Woodhead Publishing Ltd and CRC Press LLC, Cambridge & Newyork.

45. Hearle, J. W. S., & Zhou, C. Y., (1987), *Tensile Properties of Twisted para-Aramid Fibers*, Textile Research Journal, 57(1), 7-13.

46. Azpitarte, I., Zuzuarregui, A., Ablat, H., Ruiz-Rubio, L., Lopez-Ortega, A., Elliott, S. D., & Knez, M., (2017), *Suppressing the thermal and ultraviolet sensitivity of Kevlar by infiltration and hybridization with ZnO*, Chemistry of Materials, 29(23), 10068-10074.

47. Houshyar, S., Padhye, R., Nayak, R., & Shanks, R. A., (2016), *Deterioration of polyaramid and polybenzimidazole woven fabrics after ultraviolet irradiation*, Journal of Applied Polymer Science, 133(9).

48. Liu, X., Yu, W., & Pan, N., (2011), *Evaluation of high performance fabric under light irradiation*, Journal of Applied Polymer Science, 120(1), 552-556.

49. Dong, L., Shi, M., Xu, S., Sun, Q., Pan, G., Yao, L., & Zhu, C., (2020), *Surface construction of fluorinated TiO 2 nanotube networks to develop uvioresistant superhydrophobic aramid fabric*, RSC advances, 10(38), 22578-22585.

50. Mosquera, M. E., Jamond, M., Martinez-Alonso, A., & Tascon, J. M., (1994), *Thermal transformations of Kevlar aramid fibers during pyrolysis: infrared and thermal analysis studies*, Chemistry of materials, 6(11), 1918-1924.

51. Chu, Y., Chen, C., Huang, W., Li, S., Rahman, R., Min, S., ... & Chen, X., (2023), *Growing ZnO nanowires on aramid fabric for improving the ultraviolet aging property*, Textile Research Journal, 93(1-2), 280-290.

52. Almaroof, A., Ali, A., Mannocci, F., & Deb, S., (2019), *Semi-interpenetrating network composites reinforced with Kevlar fibers for dental post fabrication*, Dental materials journal, 38(4), 511-521.

53. Cheng, Z., Hong, D., Dai, Y., Jiang, C., Meng, C., Luo, L., & Liu, X., (2018), *Highly improved Uv resistance and composite interfacial properties of aramid fiber via iron (III) coordination*, Applied Surface Science, 434, 473-480.

54. Nascimento, R. F., da Silva, A. O., Weber, R. P., & Monteiro, S. N., (2020), *Influence of UV radiation and moisten associated with natural weathering on the ballistic performance of aramid fabric armor*, Journal of Materials Research and Technology, 9(5), 10334-10345.

55. Cheng, Z., Chen, C., Huang, J., Chen, T., Liu, Y., & Liu, X., (2017), *Nondestructive grafting of PEI on aramid fiber surface through the coordination of Fe ( Ⅲ) to enhance composite interfacial properties*, Applied Surface Science, 401, 323-332.

56. Arrieta, C., David, É., Dolez, P., & Vu-Khanh, T., (2011), *Hydrolytic and photochemical aging studies of a Kevlar®-PBI blend*, Polymer degradation and stability, 96(8), 1411-1419.

57. Zhang, S., Li, M., Cheng, K., & Lu, S., (2020), *A facile method to prepare PEG coatings on the fiber surface by the reconstruction of hydrogen bonds for enhancing the interfacial strength of fibers and resins*, Colloids and Surfaces A: Physicochemical and Engineering Aspects, 589, 124426.

58. Zhang, L., Kong, H., Qiao, M., Ding, X., & Yu, M., (2020), *Supercritical CO2-induced nondestructive coordination between ZnO nanoparticles and aramid fiber with highly improved interfacial-adhesion properties and UV resistance*, Applied Surface Science, 521, 146430.

59. Sathya, M., Shobika, P. A., Ponnar, M., Pushpanathan, K., & Elsi, S., (2022), *Influence of Sr concentration on crystal structure, magnetic properties and supercapacitance performance of ZnO nanoparticles*, Journal of Materials Science: Materials in Electronics, 33(9), 6745-6765.

60. Suwanboon, S., (2008), *Structural and optical properties of nanocrystalline ZnO powder from sol-gel method*, Science Asia, 34(1), 31-34.

61. Shao, L., Zhang, L., Chen, M., Lu, H., & Zhou, M., (2001), *Reactions of titanium oxides with water molecules. A matrix isolation FTIR and density functional study*, Chemical physics letters, 343(1-2), 178-184.

62. Davis, R., Chin, J., Lin, C. C., & Petit, S., (2010), *Accelerated weathering of polyaramid and polybenzimidazole firefighter protective clothing fabrics*, Polymer Degradation and Stability, 95(9), 1642-1654.

63. Santos, T., Santos, C., Aquino, M., Rangappa, S. M., Siengchin, S., Nascimento, J. H. O., & Medeiros, I., (2023), *Effects of UV sensitivity and accelerated photo-aging on stab resistance of ρ-aramid fabrics impregnated with shear thickening fluids (STFs)*, Heliyon, 9(4).

64. Li, M., Cheng, K., Wang, C., & Lu, S., (2021), *Functionalize aramid fibers with polydopamine to possess UV resistance*, Journal of Inorganic and Organometallic Polymers and Materials, 31(7), 2791-2805.

65. Zhang, J., & Teng, C., (2020), *Nondestructive growing nano-ZnO on aramid fibers to improve UV resistance and enhance interfacial strength in composites*, Materials & Design, 192, 108774.

66. Wang, B., Duan, Y., & Zhang, J., (2016), *Titanium dioxide nanoparticles-coated aramid fiber showing enhanced interfacial strength and UV resistance properties*, Materials & Design, 103, 330-338.

67. Patterson, B. A., & Sodano, H. A., (2016), *Enhanced interfacial strength and UV shielding of aramid fiber composites through ZnO nanoparticle sizing*, ACS Applied Materials & Interfaces, 8(49), 33963-33971.

68. Xing, Y., & Ding, X., (2007), *UV photo‑stabilization of tetrabutyl titanate for aramid fibers via sol–gel surface modification*, Journal of applied polymer science, 103(5), 3113-3119.